Environmental Science & Technology Letters

Letter

Cite This: Environ. Sci. Technol. Lett. 2017, 4, 470-474

pubs.acs.org/journal/estlcu

A Combined Heat- and Power-Driven Membrane Capacitive Deionization System

Jiankai Zhang,[†] Kelsey B. Hatzell,[‡] and Marta C. Hatzell*[,†]

[†]George W. Woodruff School of Mechanical Engineering, Georgia Institute of Technology, Atlanta, Georgia 30313, United States

[‡]Department of Mechanical Engineering, Vanderbilt University, Nashville, Tennessee 401592, United States

Supporting Information

ABSTRACT: Here, we experimentally investigate an alternative membrane capacitive deionization (MCDI) system cycle, which aims to reduce the required electrical energy demand for water treatment. The proposed heat and power combined MCDI system utilizes waste heat to control the electrostatic potential of the charged electrodes during the charging (desalination) and discharging (energy recovery) processes. The experimental findings suggest that with an increase in the temperature of the brine from 20 to 50 °C, the electrical energy consumed can be reduced by nearly 10%. We also show that the dependence of electrostatic potential on concentration may limit energy recovery performance (power), when moving toward higher water recoveries. Alternative desalination cycles can be further explored through evaluating non-isothermal and non-adiabatic system operation.

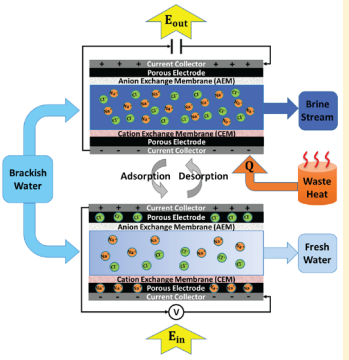

INTRODUCTION

Managing energy consumption during water treatment processes and water use during energy generation is a critical component of the water−energy nexus.[1] Thermoelectric power plants account for 38% of fresh water withdrawals in the United States, and a majority of this water is used for on-site cooling (≈80%) and power generation (≈10%).[2,3] Technologically, dry cooling could aid in minimizing the demand for water during cooling, and low-energy water treatment technologies could reduce the amount of energy spent on boiler water treatment. Furthermore, improvements made in treating boiler water have a direct impact on improving plant thermal efficiencies, as high total dissolved solids (TDS) result in a low rate of heat transfer due to corrosion and fouling.[4] Boiler water treatment will become increasingly important because high-efficiency super-critical based power plants require more stringent water quality.[4]

Treating water to pure and ultrapure levels can be energy intensive and traditionally requires treatment strategies that combine softening with multiple passes through a reverse osmosis (RO) system. Most energy generation and industrial sites that require pure water also have access to an abundance of waste heat, which could act as an ideal free energy source for water treatment.[5] Therefore, developing synergistic approaches to use this "waste energy" source has become desirable. Currently, indirect and direct means for converting low-grade waste heat into deionized water do exist. Indirect approaches include those that convert heat to power through technologies such as thermoelectric devices and then use that power to operate a water treatment system.[6] While possible, undesirable energy conversion losses, larger system footprints, and cost typically limit their practical implementation.

Direct utilization of thermal energy can be accomplished through thermal and membrane distillation,[7,8] yet thermal efficiencies remain low, especially with low-grade waste heat sources.[9] Traditional membrane processes cannot yet effectively capture heat as a driving force for enhanced separations due to increased rates of fouling;[10] however, forward osmosis has captured thermal energy to augment desalination through the use of draw solutions that are regenerated using thermal energy.[11−13]

Here, we aim to detail a process for harvesting thermal energy within an electrochemically driven deionization system termed membrane capacitive deionization (MCDI). MCDI offers several advantages for effective brackish water treatment (low specific energy consumption), yet is purely driven by electrical energy.[14] We experimentally investigate the potential for harvesting thermal energy through exploiting the electrostatic and membrane potentials dependence on temperature. We also highlight the role heat plays in limiting losses that arise when moving MCDI toward high-water recovery operating conditions.

EXPERIMENTAL METHODS

Experimental Setup. The actual MCDI cell consists of two insulated polycarbonate end plates, two titanium current collectors, two activated carbon electrodes (2 cm^2), two membranes (Selemion, AMV, and Selemion CMV, δ = 110

Received: September 7, 2017
Revised: September 30, 2017
Accepted: October 2, 2017
Published: October 2, 2017

DOI: 10.1021/acs.estlett.7b00395
Environ. Sci. Technol. Lett. 2017, 4, 470−474

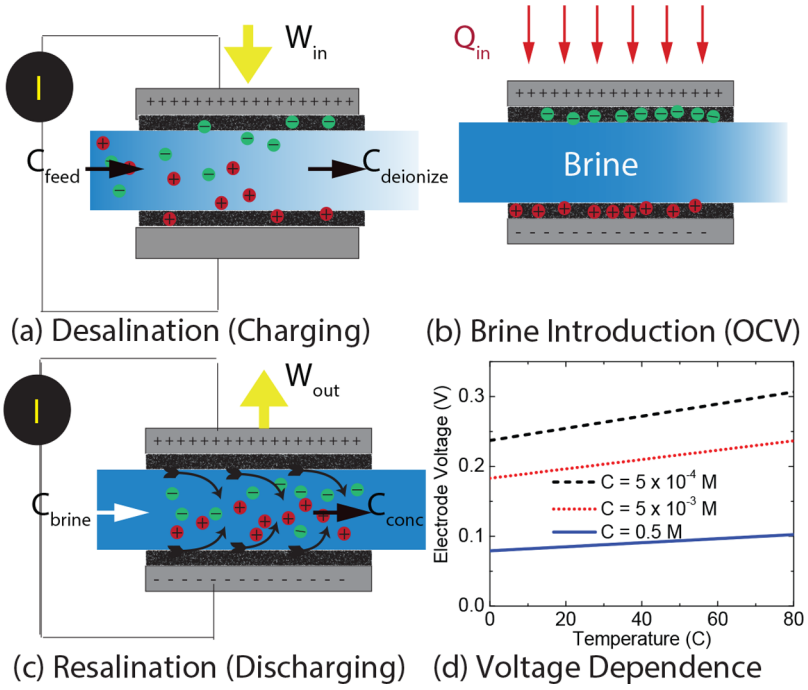

Figure 1. Three-stroke desalination process with (a) the desalination (charging) step followed by (b) brine introduction (OCV) with heat addition and (c) resalination (discharge). (d) Dependence of the electric double-layer voltage on temperature and concentration at a fixed charge density.

μm, AGC Engineering), and one silicone gasket (δ = 1 mm, McMaster-Carr) which have the flow channel. The cation and anion exchange membrane (CEM and AEM) were placed in front of the activated carbon free-standing films. MCDI tests are performed in batch mode with a separate feed and brine solution recycled at a rate of 10 mL/min during desalination and brine formation processes. The brine reservoir was situated on a hot plate, which allowed for control over the water (feed/brine) temperature. The conductivity values are measured for the bulk solution, using an Orion Versa Star conductivity probe and meter (Fisher Scientific).

Electrochemical Characterization. The effects of temperature and salt concentration on MCDI properties were electrochemically characterized by cyclic voltammetry (CV) and electrochemical impedance spectroscopy (EIS). We perform CV experiments on the CDI cell without membranes when evaluating the electrode capacitance. The voltage was swept in a range from −1.0 to 1.0 V at two scan rates (ν = 2 and 10 mV/s). From the CV diagrams, the specific gravimetric C_{sp} (farads per gram), the capacitance per mass of activated carbon electrode, was calculated by the following equation.

$$C_{sp} = \frac{2}{\nu m \Delta U} \int i \, dU \tag{1}$$

where m is the mass of one electrode, i is the electrical current, and ΔU is the voltage window. The standing film electrodes utilized during electrochemical characterization and MCDI experiments were 2 cm^2 and 50 mg.

EIS is used to determine the capacitive and resistive elements of electrode−electrolyte interface properties. The Nyquist diagrams of the MCDI cell under different operational conditions (salt concentration and temperature) are generated within the frequency range from 200 kHz to 10 mHz. At a high frequency, the initial intercept represents internal resistance R_s, including ohmic resistance from electrodes, membranes, and the electrolyte. The semicircle provides the information regarding charge transfer resistance R_{CT} and double-layer capacitance C_{DL}. To quantitatively evaluate resistive and capacitive elements, an electrical-circuit model is used to simulate the experimental data. All EIS fitted data is provided in the Supporting Information.

Energy Analysis. The salt ion adsorption−desorption cycles in MCDI proceed by applying a constant current (chronopotentiometry). While the ion adsorption process requires that electrical energy be added to the system, during discharge a portion of the energy can be recovered. To evaluate the net electrical work in experiments, a constant-current method was implemented on both charging and discharging steps, and an open-circuit voltage (OCV) mode was introduced between the steps (Figures 2a and 3a). The cell voltage response is recorded throughout this three-stroke intermittent cycle. On the basis of the experimental measurements, the energy consumed and recovered (E_c and E_d) is calculated by integrating the power over the time period of ion adsorption and desorption. Given that the charging current (I_c) and discharge current (I_d) remained constant, the net electrical energy (E_{net}) throughout the cycle is computed via eq 2.

$$E_{net} = E_c - E_d = I_c \int_{t_{c,i}}^{t_{c,f}} V \, dt - I_d \int_{t_{d,i}}^{t_{d,f}} V \, dt \tag{2}$$

where $t_{c,i}$ and $t_{c,f}$ denote the moments that constant current is applied and removed during the charging step, and $t_{d,i}$ and $t_{d,f}$ represent the start and ending time during discharge. All energetics were evaluated by characterizing mulitple cycles (5) under identical conditions. Future work will aim to evaluate stability over longer operational periods. Additional methods and theory are provided in the Supporting Information.

RESULTS AND DISCUSSION

A membrane capacitive deionization (MCDI) desalination cycle consists of a three-stroke process. Electrodes are charged in a feed solution (C_{feed} < 0.1 M), producing a deionized stream

DOI: 10.1021/acs.estlett.7b00395
Environ. Sci. Technol. Lett. 2017, 4, 470−474

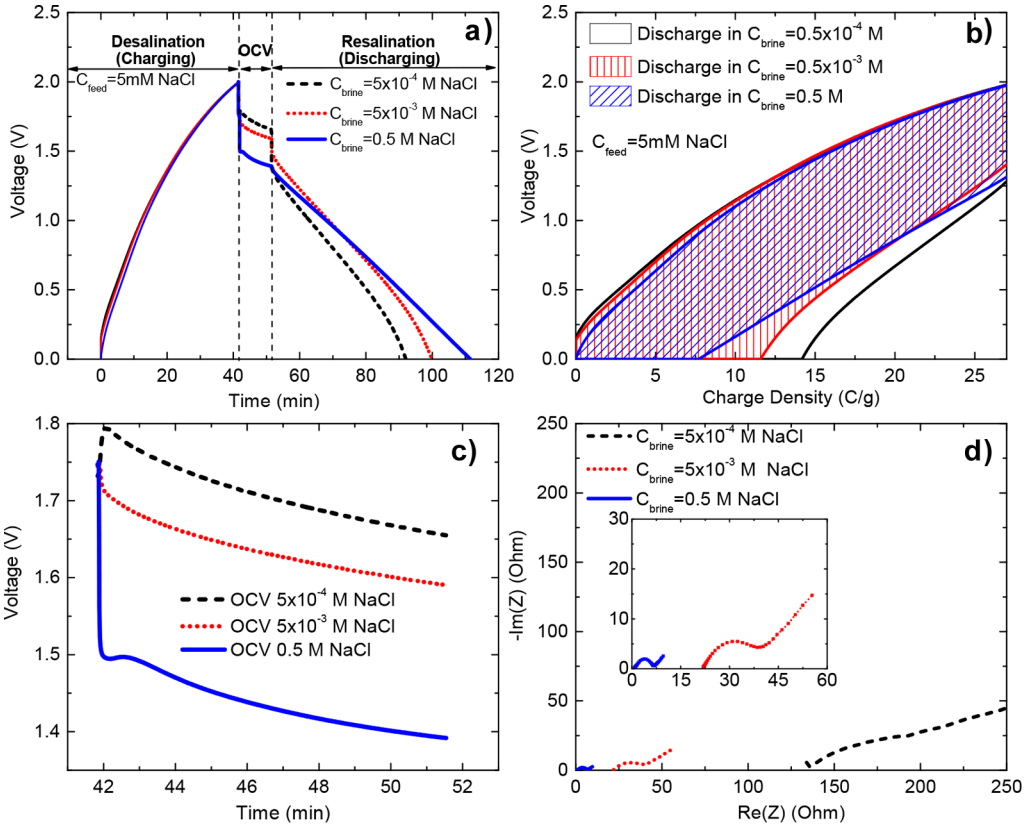

Figure 2. Adiabatic three-step desalination cycle with a C_{feed} of 5×10^{-3} M (T_{feed} = 20 °C) and C_{brine} values of 5×10^{-4}, 5×10^{-3}, 0.5 M NaCl (T_{brine} = 20 °C). (a) Charge−discharge behavior. (b) Voltage vs charge density (V−σ). (c) Open-circuit voltage. (d) EIS Nyquist plots.

(C_d), and then a brine is introduced into the cell (usually under an open circuit). Next, the electrodes are regenerated while a concentrated stream is produced (Figure 1a−c). Most MCDI cells operate under conditions that produce 50% water recovery ($V_{deionized}/V_{feed}$ = 50%).[15] In reality, higher water recoveries on the order of 90% are desirable to limit the volume of waste produced (V_{conc}) and maximize the volume of clean water ($V_{deionized}$). If high water recoveries are desirable, the brine concentration should increase,[16] compared to what is currently being reported in the literature. This will have a beneficial effect on the electrochemical performance of the system due to a reduction in ohmic losses (approximately −500 mV), but this improvement is reduced by a decrease in the electric double-layer voltage (≈200−300 mV) (Figure 1d). Here, we will discuss an alternative three-stroke MCDI desalination cycle that includes a non-adiabatic brine heating stage (Figure 1b) prior to discharge. The non-adiabatic heat addition serves two purposes: (1) to minimize the voltage drop that arises due to the high-salinity brine and (2) to integrate thermal energy recovery during water treatment.

Effect of the Brine Salt Concentration. Here, a MCDI cell was charged in a 5 mM feed solutions to 2 V under a constant current and discharged in various brines (5×10^{-4}, 5×10^{-3}, and 0.5 M NaCl) (Figure 2a). During stroke 1, the desalination performance of all cells was identical because of the constant current operation. However, when the brines at various concentrations are introduced, the open-circuit resting voltage decreased as the brine concentration increased (Figure 2a,c). This is directly linked to the dependence of the EDL voltage on concentration (Supporting Information). Introducing a solution with a lower concentration ($C_{Brine} \leq C_{feed}$) produced the highest OCV due to an increase in the EDL, similar to the phenomenon exploited in the field of capacitive mixing.[17,18] The use of a real brine ($C_{Brine} \geq C_{feed}$) had the opposite effect. The high concentrations caused the EDL to compress, resulting in a lower (≈300 mV) OCV. Decreasing the OCV reduces the voltage during discharge, which results in a lower power discharge rate.

To evaluate the energy of the cycles, the cell voltage (V) is plotted with respect to the surface charge density (σ). The enclosed area represents the net electrical work required (Figure 2b). Because of the high voltage used in these tests, a significant amount of faradaic reactions resulted in a loss of charge. This is visible through the V−σ figure not returning to zero after discharge. Charging to lower voltages (≈1 V) and deaerating the solutions can aid in limiting these side reactions.[19] Despite these losses, with an increasing brine concentration (C_{brine} = 5×10^{-4}, 5×10^{-3}, and 0.5 M NaCl), the total energy consumption per unit of desalinated water decreased from 230 ± 5, 209 ± 3 to 192 ± 4 kJ m^{-3}. This decrease in energy consumption is most closely tied to the reduction in ohmic losses from 130 to 2 Ω (Figure 2d). It should be noted that the power ($P = IV$) during energy recovery was initially higher (first 10 min) for the lower saline brine despite the high ohmic resistance. However, beyond this period of time, the ohmic losses dominated energy recovery (Figure 2a,b).

Effect of Brine Temperature. To evaluate the effect heating the brine had on system performance, the same three-stroke desalination cycle executed above was performed. The only difference was that the brine concentration was fixed (C_{brine} = 0.5 M), and the brine temperature was varied between

DOI: 10.1021/acs.estlett.7b00395
Environ. Sci. Technol. Lett. 2017, 4, 470−474

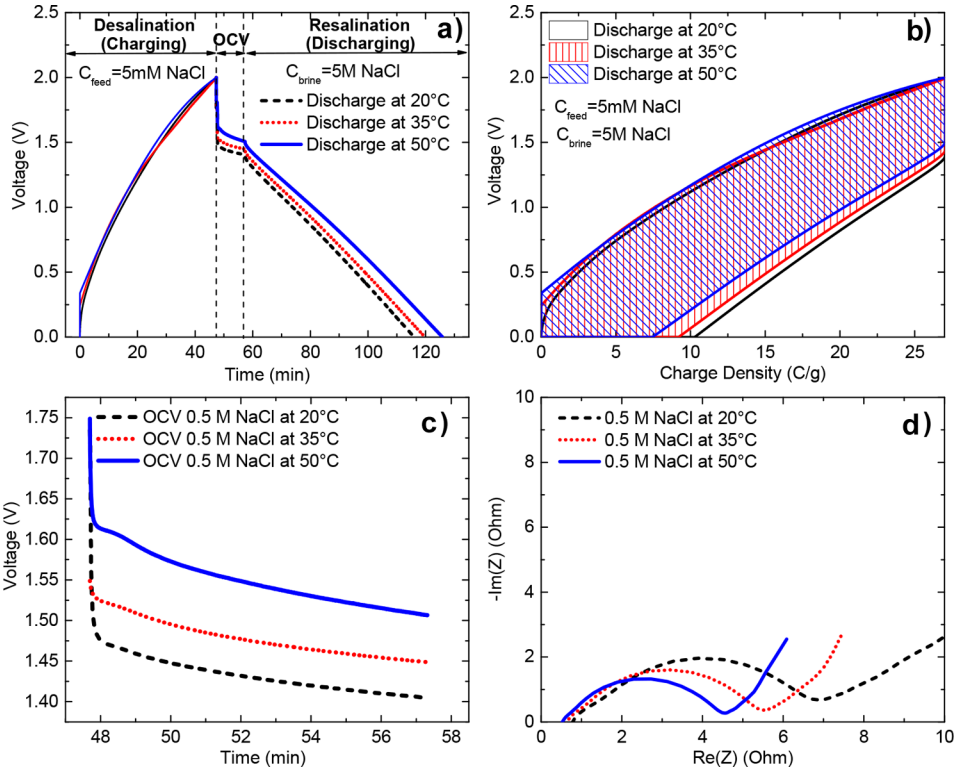

Figure 3. Non-adiabatic three-step desalination cycle with a C_{feed} of 5×10^{-3} M at 20 °C and a C_{brine} of 0.5 M at 20, 35, and 50 °C. (a) Charge–discharge behavior. (b) Voltage vs charge density ($V-\sigma$). (c) Open-circuit voltage. (d) EIS Nyquist plots.

20 and 50 °C. The temperatures were chosen to simulate various degrees of constant heat addition. Again, a constant current desalination, followed by an open-circuit brine introduction, and constant current resalination cycle was utilized. The first observation is that the voltage drop previously ascribed to the EDL compression was mitigated by nearly 150 mV as the brine temperature increased from 20 to 50 °C (Figure 3a,c). With an increase in discharge voltage, at the same ohmic performance (Figure 3c), the $V-\sigma$ curve begins to decrease in area with an increase in temperature. This reduction in area represents the reduction in electrical energy required to deionize the feed stream. Conversely, this reduction in area can be equated to work harvested from thermal energy. This is in line with a prior theory that evaluated thermodynamic cycles for capacitive mixing and CDI cells.[20] Here, electrical energy demand was further reduced from 192 ± 4 kJ m^{-3} at 20 °C to 185 ± 2 kJ m^{-3} at 35 °C and 175 ± 1 kJ m^{-3} at 50 °C. Furthermore, the voltage during the entire discharge is higher, resulting in a higher power discharge over the entire resalination stroke. The performance can be directly tied to the temperature dependence of the EDL voltage, as the measured capacitance did not change significantly with operating temperature (Figure 2a).

When thermal energy recovery systems are operated near ambient conditions, the Carnot efficiency limits thermal energy conversion to a maximum of ≈10%. Traditional waste heat to power applications such as thermoelectric devices that have existed for decades struggle to achieve even a fraction of the Carnot limit.[21] Here, this waste heat to water technology achieved 0.2% of the Carnot limit. The performance is in line with prior waste heat to power technologies,[22] despite the significant losses observed due to faradic reactions and the lack of a heat management system. Here, the entire brine solution was heated, which had a heat capacity of 4.18 kJ kg^{-1} K^{-1}. If the electrodes were directly heated, the efficiency could increased by at least 5-fold (see the Supporting Information).

CONCLUSIONS

In summary, a waste heat to water technology based around a membrane capacitive deionization device is explored. Alternative desalination cycles can be envisioned which aim to minimize the electrical work required for deionizing brackish waters, through the use of non-adiabatic and non-isothermal based processes. Here we detailed one such cycle where heat is directly harvested to exploit the electric double-layer dependence on temperature during the discharge stroke. The potential for harvesting low-grade waste heat specifically could have a unique fit for aiding in boiler water treatment, where an abundance of water must be treated and excess amount of waste heat is available.

ASSOCIATED CONTENT

Supporting Information

The Supporting Information is available free of charge on the ACS Publications website at DOI: 10.1021/acs.estlett.7b00395.

Experimental procedures and calculations (PDF)

AUTHOR INFORMATION

Corresponding Author

*E-mail: marta.hatzell@me.gatech.edu. Phone: +1 404-385-4503.

ORCID

Marta C. Hatzell: 0000-0002-5144-4969

Notes

The authors declare no competing financial interest.

DOI: 10.1021/acs.estlett.7b00395
Environ. Sci. Technol. Lett. 2017, 4, 470–474

■ ACKNOWLEDGMENTS

This material is based upon work supported by the National Science Foundation under Grant 1706290 to M.C.H. and Grant 1706956 for K.B.H. The authors thank Daniel Moreno and Mohammadreza Nazemi for helpful discussions.

■ REFERENCES

(1) Philbrick, M.; Vallario, B. *The Water-Energy Nexus: Challenges and Opportunities*; U.S. Department of Energy: Washington, DC, 2014.
(2) Maupin, M. A.; Kenny, J. F.; Hutson, S. S.; Lovelace, J. K.; Barber, N. L.; Linsey, K. S. *Estimated use of water in the United States in 2010*; U.S. Geological Survey: Reston, VA, 2014.
(3) Zhai, H.; Rubin, E. S.; Versteeg, P. L. Water use at pulverized coal power plants with postcombustion carbon capture and storage. *Environ. Sci. Technol.* **2011**, *45*, 2479−2485.
(4) Rayaprolu, K. *Boilers for power and process*; CRC Press: Boca Raton, FL, 2009.
(5) Gingerich, D. B.; Mauter, M. S. Quantity, quality, and availability of waste heat from United States thermal power generation. *Environ. Sci. Technol.* **2015**, *49*, 8297−8306.
(6) Date, A.; Gauci, L.; Chan, R.; Date, A. Performance review of a novel combined thermoelectric power generation and water desalination system. *Renewable Energy* **2015**, *83*, 256−269.
(7) Jansen, A.; Assink, J.; Hanemaaijer, J.; Van Medevoort, J.; Van Sonsbeek, E. Development and pilot testing of full-scale membrane distillation modules for deployment of waste heat. *Desalination* **2013**, *323*, 55−65.
(8) Cath, T. Y.; Adams, V. D.; Childress, A. E. Experimental study of desalination using direct contact membrane distillation: a new approach to flux enhancement. *J. Membr. Sci.* **2004**, *228*, 5−16.
(9) Szacsvay, T.; Posnansky, M. Distillation desalination systems powered by waste heat from combined cycle power generation units. *Desalination* **2001**, *136*, 133−140.
(10) Jawor, A.; Hoek, E. M. Effects of feed water temperature on inorganic fouling of brackish water RO membranes. *Desalination* **2009**, *235*, 44−57.
(11) McCutcheon, J. R.; McGinnis, R. L.; Elimelech, M. Desalination by ammonia-carbon dioxide forward osmosis: influence of draw and feed solution concentrations on process performance. *J. Membr. Sci.* **2006**, *278*, 114−123.
(12) McGinnis, R. L.; Elimelech, M. Energy requirements of ammonia-carbon dioxide forward osmosis desalination. *Desalination* **2007**, *207*, 370−382.
(13) Zhou, X.; Gingerich, D. B.; Mauter, M. S. Water treatment capacity of forward-osmosis systems utilizing power-plant waste heat. *Ind. Eng. Chem. Res.* **2015**, *54*, 6378−6389.
(14) Oren, Y. Capacitive deionization (CDI) for desalination and water treatment-past, present and future (a review). *Desalination* **2008**, *228*, 10−29.
(15) Biesheuvel, P. Thermodynamic cycle analysis for capacitive deionization. *J. Colloid Interface Sci.* **2009**, *332*, 258−264.
(16) García-Quismondo, E.; Santos, C.; Soria, J.; Palma, J.; Anderson, M. A. New operational modes to increase energy efficiency in capacitive deionization systems. *Environ. Sci. Technol.* **2016**, *50*, 6053−6060.
(17) Brogioli, D. Extracting renewable energy from a salinity difference using a capacitor. *Phys. Rev. Lett.* **2009**, *103*, 058501.
(18) Hatzell, M. C.; Hatzell, K. B.; Logan, B. E. Using flow electrodes in multiple reactors in series for continuous energy generation from capacitive mixing. *Environ. Sci. Technol. Lett.* **2014**, *1*, 474−478.
(19) He, D.; Wong, C. E.; Tang, W.; Kovalsky, P.; Waite, T. D. Faradaic reactions in water desalination by batch-mode capacitive deionization. *Environ. Sci. Technol. Lett.* **2016**, *3*, 222−226.
(20) Janssen, M.; Härtel, A.; Van Roij, R. Boosting capacitive blue-energy and desalination devices with waste heat. *Phys. Rev. Lett.* **2014**, *113*, 268501.
(21) Vining, C. B. An inconvenient truth about thermoelectrics. *Nat. Mater.* **2009**, *8*, 83.
(22) Sales, B. B.; Burheim, O. S.; Porada, S.; Presser, V.; Buisman, C. J.; Hamelers, H. V. Extraction of energy from small thermal differences near room temperature using capacitive membrane technology. *Environ. Sci. Technol. Lett.* **2014**, *1*, 356−360.

DOI: 10.1021/acs.estlett.7b00395
Environ. Sci. Technol. Lett. 2017, 4, 470−474